

Article

Design, Synthesis and Biological Evaluation of 6-(2,6-dichloro-3,5-dimethoxyphenyl)-4-Substitute d-1*H*-indazoles as Potent Fibroblast Growth Factor Receptor Inhibitors

Zhen Zhang^{1,2}, Dongmei Zhao^{1,*}, Yang Dai³, Maosheng Cheng¹, Meiyu Geng³, Jingkang Shen², Yuchi Ma^{2,*}, Jing Ai^{3,*}, Bing Xiong^{2*}

¹ Key Laboratory of Structure-Based Drug Design & Discovery of Ministry of Education, Shenyang Pharmaceutical University, Shenyang 110016, P. R. China

² Department of Medicinal Chemistry, State Key Laboratory of Drug Research, Shanghai Institute of Materia Medica, Chinese Academy of Sciences, 555 Zuchongzhi Road, Shanghai 201203, China

³ Division of Anti-tumor Pharmacology, State Key Laboratory of Drug Research, Shanghai Institute of Materia Medica, Chinese Academy of Sciences, 555 Zuchongzhi Road, Shanghai 201203, China

*Corresponding authors. (B. Xiong.) Tel: +86 21 50806600 ext. 5412 fax: +86 21 50807088. Email: bxiong@simm.ac.cn; (J. Ai) Tel: +86 21 50806600 ext. 2413. Email: jai@simm.ac.cn; (D. Zhao) Fax: +86-24-23995043; Tel: +86-24-23986413 Email: dongmeiz-67@163.com; (Y. Ma.) Tel: +86 21 50806600 ext. 5412 fax: +86 21 50807088. Email: yhma@simm.ac.cn;

Abstract:

Tyrosine kinase fibroblast growth factor receptor (FGFR), which is aberrant in various cancer types, is a promising target for cancer therapy. Here we reported the design, synthesis, and biological evaluation of a new series of 6-(2,6-dichloro-3,5-dimethoxyphenyl)-4-substituted-1*H*-indazoles derivatives as potent FGFR inhibitors. Compound **10a** was first identified as a potent FGFR1 inhibitor, with good enzymatic inhibition. Further structure-based optimization revealed that compound **13a** is the most potent FGFR1 inhibitor in this series with the enzyme inhibitory activity about 30.2 nM of IC₅₀ value.

Keywords: Cancer; FGFR; Inhibitor; 4-Substituted-1*H*-indazole

1. Introduction

Fibroblast growth factor receptors (FGFRs), consisting of four members FGFR1-4, belong to the family of receptor tyrosine kinases (RTKs) and play fundamental roles in several basic biological processes, including tissue development, angiogenesis and tissue regeneration [1-3]. Over-activation of FGFR signaling has occurred in many types of cancers due to gene amplification, mutation or translocations [4-7]. Aberrant FGFR signaling drives oncogenic growth of tumor subsets, especially those lacking effective treatments, such as 20% squamous non-small cell lung carcinoma and 4% triple-negative breast cancer, etc [8-11]. Therefore, FGFR has been validated as an attractive target for targeted cancer therapy [8,12-14].

In recent years, several small molecular FGFR inhibitors have been reported, and some of them are now in clinical trials [15]. The early examples of FGFR inhibitors are predominantly multi-targeted, such as nintedanib, lenvatinib, dovitinib, and lucitanib [16]. Although simultaneous inhibition of multiple RTKs may reinforce the efficacy in patients by concomitant disturbance of redundant pathways, it may also increase the chance of side effects or severe toxicity [17,18]. Thus, discovery of potent and selective FGFR inhibitors is an urgent need in cancer treatment. Currently, several FGFR-selective inhibitors have progressed into clinical trials (Figure 1) [19-21]. JNJ-42756493 (**1**) is a potent oral pan-FGFR inhibitor with

IC₅₀ values in the low nanomolar range for FGFR1-4 and it was effective in vitro and in vivo in CRC tumors such as cell line NCI-H716 harboring amplified FGFR2 [19]. AZD4547 (**2**) is a highly potent and selective FGFR1-3 inhibitor. During the phase I trial, on-target activity was observed in 5 of 20 patients with tumors harboring FGFR signaling aberrations. Better Efficacy was shown in patients with a high level of FGFR amplification [20]. NVP-BGJ398 (**3**), currently in phase II clinical trials, inhibits FGFR1-4 with low nanomolar potency at the molecular level (IC₅₀ = 0.9, 1.4, 1.0, and 60 nM, respectively) and demonstrated at least 200-fold selectivity for FGFRs over other evaluated kinases [21].

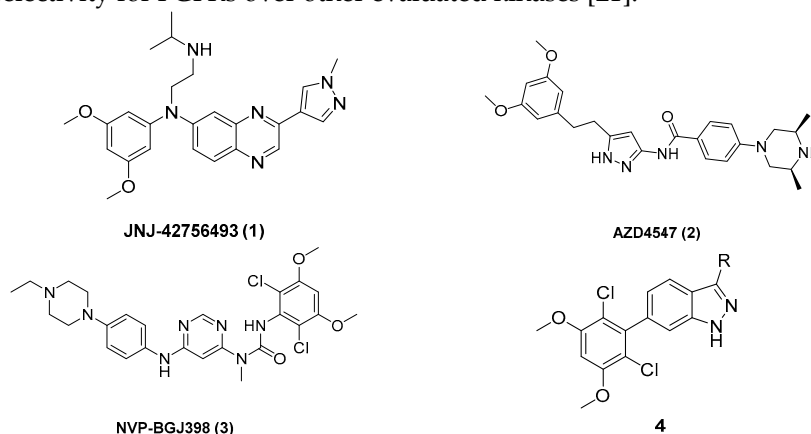


Fig.1 Structure of the representative selective FGFR inhibitors.

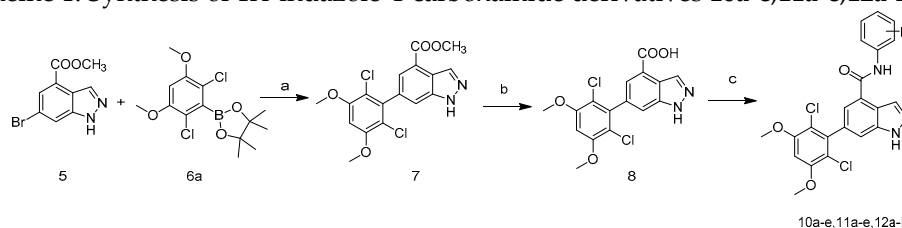
Recently, several series of 6-(2,6-dichloro-3,5-dimethoxyphenyl)-1*H*-indazole compounds (**4**) as FGFR inhibitors were reported [22,23]. Based on this promising scaffold and excellent bioactivity, we continued to investigate this chemotype in detail. Since the reported 6-(2,6-dichloro-3,5-dimethoxyphenyl)-1*H*-indazole compounds all focused on the optimization at C3-position of indazole that extends into solvent part in the FGFR binding site, we were wondering whether other position can be utilized to increase the binding activity. By taking advantage of docking studies, we hypothesized that the C4-position of indazole may be a new direction for optimization, as it can extend into a new binding subpocket in ATP site of FGFR. Therefore, we designed and synthesized a new series of FGFR inhibitors containing 6-(2,6-dichloro-3,5-dimethoxyphenyl)-1*H*-indazole scaffold, and the FGFR1 enzymatic evaluation indeed showed the good bioactivity of this series of inhibitors.

2. Results and Discussion

2.1 Chemistry

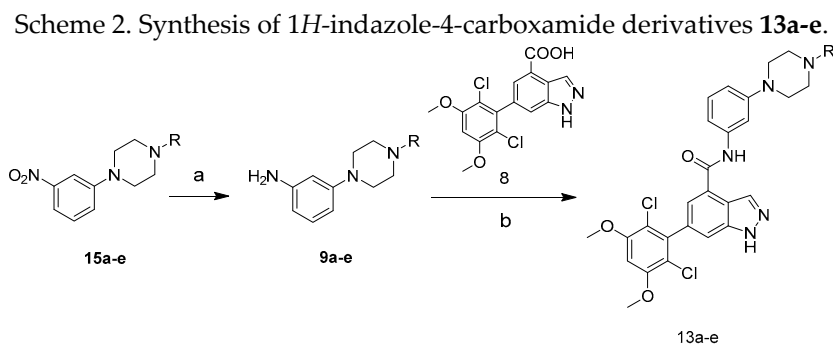
Compounds **10a-e**, **11a-e**, **12a-i** were prepared according to the procedure shown in Scheme 1. Suzuki coupling of methyl 6-bromo-1*H*-indazole-4-carboxylate (**5**) with 2-(2,6-dichloro-3,5-dimethoxyphenyl)-4,4,5,5-tetramethyl-1,3,2-dioxaborolane (**6a**) provided methyl 6-(2,6-dichloro-3,5-dimethoxyphenyl)-1*H*-indazole-4-carboxylate (**7**). Treatment of compound **7** with lithium hydroxide afforded 6-(2,6-dichloro-3,5-dimethoxyphenyl)-1*H*-indazole-4-carboxylic acid (**8**). Compounds **10a-e**, **11a-e**, **12a-i** were prepared by subjecting compound **8** to condensation with the appropriate aromatic amine derivatives.

Scheme 1. Synthesis of 1*H*-indazole-4-carboxamide derivatives **10a-e**, **11a-e**, **12a-i**.



Reagents and conditions: (a) i) Boc_2O , Cs_2CO_3 , 1,4-Dioxane, r.t., 0.5h; ii) 2-(2,6-dichloro-3,5-dimethoxyphenyl)-4,4,5,5-tetramethyl-1,3,2-dioxaborolane, $\text{Pd}(\text{dppf})\text{Cl}_2$, 1,4-Dioxane: H_2O = 3:1, 100 °C, 2 h, 62.3%; (b) $\text{LiOH}\cdot\text{H}_2\text{O}$, THF, 50°C, 6h, 76.2%; (c) i) POCl_3 , pyridine, 0°C, 1h; ii) aniline, 0°C, 10min; iii) r.t., 1.5h, 60.5%-82.3%.

Compounds **13a-e** were prepared according to the procedure shown in Scheme 2. Commercially available **15a-e** were performed the reduction reaction with iron powder to afford 3-(4-substituted-piperazin-1-yl)aniline (**9a-e**). Compound **13a-e** were prepared by compound **8** condensation with the **9a-e**.



Reagents and conditions: (a) Fe, NH_4Cl , Ethanol, 80°C, 2-6h, 35.5%-55.1%; (b) HATU, DIPEA, DCM, r.t., 3h, 55.6%-65.8%.

2.2 Inhibitor Design

To elucidate the interaction of 6-(2,6-dichloro-3,5-dimethoxyphenyl)-1*H*-indazole scaffold (**4**) with FGFR, we performed a docking study on the compound **4** in the ATP site of FGFR1 using a reported crystal structure of the FGFR1 kinase domain (PDB ID: 3TT0), as shown in Figure 2A. According to this model, the NH at the N1-position of 1*H*-indazole is involved in a critical H-bond with the carbonyl of GLU562, and N2 atom of indazole ring is formed another hydrogen bond with residue ALA564 located at the hinge region of the ATP-binding pocket. In addition, the two chlorine atoms, which formed favorable hydrophobic contact with Val561 and Ala640 respectively, enforced the tetra-substituted phenyl ring to adopt an almost perpendicular orientation with respect to the plane of the indazole ring. Overall the tetra-substituted phenyl ring superimposes well with the NVP-BGJ398 in co-crystal structure 3TT0. Through detailed analysis of predicted bound conformation of compound **4**, it was clear that C3 of indazole is an obvious direction for optimization as indicated by the NVP-BGJ398. We also noticed that the methyl group at amide moiety of NVP-BGJ398 is pointing to a subpocket, which also could be utilized for optimization. Therefore, we designed compound **10a** and docked it into the FGFR1 binding site. As shown in Figure 2B, the 6-(2,6-dichloro-3,5-dimethoxyphenyl)-1*H*-indazole scaffold still remains at the same position by forming essential interactions described before, while the substituted benzyl amide group extends upward into a subpocket. Considering this interesting binding mode, we synthesized this compound and evaluated its activity in the FGFR1 enzymatic assay. The result confirmed that this compound (**10a**) has good activity. Then, we selected compound **10a** as the starting point for further modification.

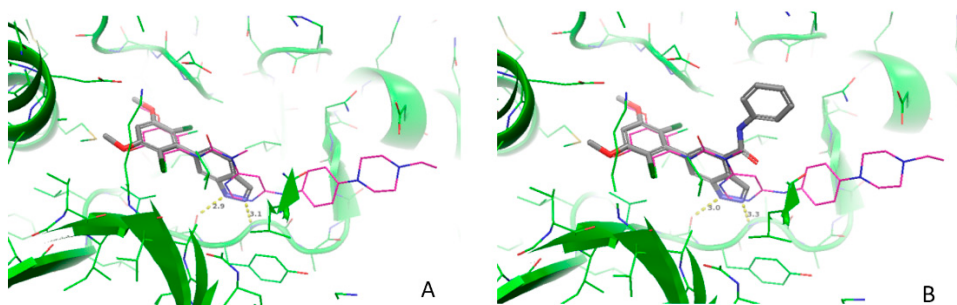
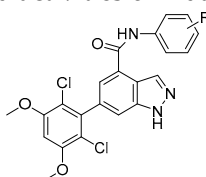


Fig. 2 The predicted binding conformation of compound 4 (A) and 10a (B) in the ATP binding site of FGFR1 based on the docking studies.

2.3 The structure–activity relationship of indazole derivatives

We first examined the impact of substitutions at the *meta*-position or *para*-position of the phenyl ring of compound 10a on their biological activity against FGFR1 (Table 1). Comparing with compound 10a, introducing acetyl (10b) at the *meta*-position of phenyl ring caused a slight increase in inhibitory activity, while introducing acetyl at the *para*-position (10c) decreased the inhibitory activity. This trend is also reflected from the pair compounds with methoxyl at the *meta*-position (10d) and *para*-position (10e). This might imply that substitution of the *meta*-position of phenyl ring could form favorable interactions with the binding site.

Table 1 Structures and activities of indazole derivatives 10a-e

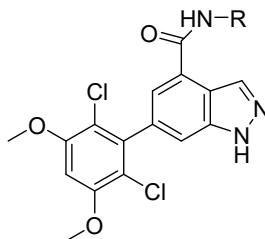


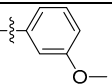
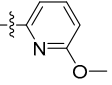
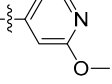
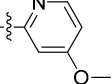
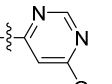
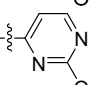
Compound No	R	Enzyme inhibition(%) ^a	
		1 μmol/L	0.1 μmol/L
10a	H	84.1	58.8
10b	<i>m</i> -acetyl	82.4	76.4
10c	<i>p</i> -acetyl	52.9	32.2
10d	<i>m</i> -methoxyl	78.4	57.0
10e	<i>p</i> -methoxyl	68.5	11.9

^aThe IC₅₀ value of AZD4547 is 1.8±0.1 nM(mean±SD).

The designed and synthesized compounds (11a-e) with modifications on phenyl moiety of compound 10d were assessed for their FGFR1 inhibitory activity (Table 2). The result indicated that replacement of the phenyl ring (10d) with pyridines (11a, 11b, 11c) or pyrimidines (11d, 11e) slightly decreased the activity.

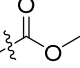
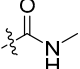
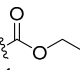
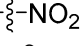
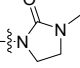
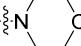
Table 2 Structures and activities of indazole derivatives 11a-e

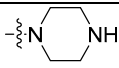
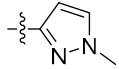
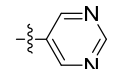


Compound No	R	Enzyme inhibition(%)	
		1 $\mu\text{mol/L}$	0.1 $\mu\text{mol/L}$
10d		78.4	57.0
11a		79.2	47.2
11b		84.3	49.5
11c		80	42.3
11d		78.5	43.1
11e		57.4	31

According to the obtained structure-activity relationship, we prepared various substitutions at the C3-position of phenyl ring (**12a-i**) and evaluated in the enzymatic assay (Table 3). Incorporation of methoxycarbonyl (**12a**), ethoxycarbonyl (**12b**), nitro group (**12d**), and 3-methyl-2-oxoimidazolidin-1-yl (**12e**) reduced enzymatic potency. Fortunately, compound containing methylcarbamoyl at 3-position of phenyl (**12b**, $\text{IC}_{50}=38.6\pm 0.2$ nM) showed better inhibitory activity than **10a** ($\text{IC}_{50}=69.1\pm 19.8$ nM). Meanwhile, it was also found that incorporation of morpholine (**12f**) and piperazine (**12g**) could retain the enzymatic potency. However, compounds containing aromatic structures at the *meta*-position of phenyl substantially reduced the inhibitory activities.

Table 3 Structures and activities of indazole derivatives **12a-i**

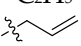
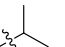
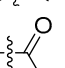
Compound No	R	Enzyme inhibition(%)		IC_{50} (nM) ^a
		0.1 $\mu\text{mol/L}$	0.01 $\mu\text{mol/L}$	
10a	H	58.8	27.3	69.1 \pm 19.8
12a		35.7	17.1	/
12b		62.3	42.1	38.6 \pm 0.2
12c		36.8	9.9	/
12d		31.6	17.4	/
12e		36.7	17.2	/
12f		58.7	28.3	54.0 \pm 8.7

12g		60.9	45.1	78.8±14.2
12h		52.7	34.5	102.9±0.6
12i		60.3	35.1	86.2±17.0

^a The IC₅₀ or inhibition values shown as the mean±SD (nM) are calculated from two separate experiments.

In order to further improve the enzymatic potency of this series of compounds against FGFR1, various groups were incorporated at the 4'-position of piperazine of compound **12g** (Table 4). Compared to **12g**, most of the resulting analogues (**13b**, **13c**, **13d**, **13e**) diminished the enzymatic activities. Nevertheless, 4-methylpiperazine analogue (**13a**, IC₅₀=30.2±1.9 nM) demonstrated excellent inhibitory activity in the enzymatic assay.

Table 4 Structures and activities of indazole derivatives **13a-e**

Compound No	R	Enzyme inhibition(%)		IC ₅₀ (nM) ^a
		0.1 μmol/L	0.01 μmol/L	
12g	H	60.9	45.1	78.8±14.2
13a	-CH ₃	72.7	48.3	30.2±1.9
13b	-C ₂ H ₅	26.4	13.7	328.4±65.7
13c		41.3	35.7	463.9±99.1
13d		18.5	7.2	/
13e		64.7	27.7	117.9±3.9

^a The IC₅₀ or inhibition values shown as the mean±SD (nM) are calculated from two separate experiments.

3. Experimental Section

3.1 Chemistry

¹H NMR (400 MHz) spectra were recorded by using a Varian Mercury-400 High Performance Digital FT-NMR spectrometer with tetramethylsilane (TMS) as an internal standard. ¹³C NMR (125 MHz) spectra were recorded by using a Varian Mercury-500 High Performance Digital FT-NMR spectrometer. Abbreviations for peak patterns in NMR spectra: s = singlet, d = doublet, and m = multiplet. Low-resolution mass spectra were obtained with a Finnigan LCQ Deca XP mass spectrometer using a CAPCELL PAK C18 (50mm × 2.0mm, 5 ZM) or an Agilent ZORBAX Eclipse XDB C18 (50mm×2.1m, 5 ZM) in positive or negative electrospray mode. Low-resolution mass spectra and high-resolution mass spectra were recorded at an ionizing voltage of 70 eV on a Finnigan/MAT95 spectrometer. Purity of all compounds was determined by analytical Gilson high-performance liquid chromatography (HPLC) using an YMC ODS3 column (50 mm × 4.6 mm, 5 ZM). Conditions were as follows: CH₃CN/H₂O eluent at 2.5 mL·min⁻¹ flow [containing 0.1% trifluoroacetic acid (TFA)] at 35 °C, 8 min, gradient 5% CH₃CN to 95% CH₃CN, monitored by UV absorption at 214 nm and 254 nm. TLC analysis was carried out with glass precoated silica gel GF254 plates. TLC spots were visualized under UV light. Flash column chromatography was performed with a Teledyne ISCO CombiFlash Rf system. All solvents and reagents were used directly as obtained commercially unless

otherwise noted. Anhydrous dimethylformamide was purchased from Acros and was used without further drying. All air and moisture sensitive reactions were carried out under an atmosphere of dry Argon with heat-dried glassware and standard syringe techniques.

3.1.1. Synthesis of

2-(2,6-dichloro-3,5-dimethoxyphenyl)-4,4,5,5-tetramethyl-1,3,2-dioxaborolane (**6a**).

To a solution of 2-(3,5-dimethoxyphenyl)-4,4,5,5-tetramethyl-1,3,2-dioxaborolane (**6**) (15 g, 56.82 mmol) in DMF (300 mL), NCS (16.7 g, 125.0 mmol) was added and the mixture was stirred at 90°C for 2 h. The reaction was cooled to 25°C and quenched with distilled water. The solid product was filtered off, washed with water, and dried (92%). ¹H NMR (400 MHz, Chloroform-*d*) δ 6.56 (s, 1H), 3.91 (s, 6H), 1.45 (s, 12H); ¹³C NMR (126 MHz, Chloroform-*d*) δ 153.73 (C×2), 116.32, 98.39(C×2), 84.55 (C×2), 56.13 (C×2), 24.30 (C×4); (+) ESI-MS *m/z* 334 [M + H]⁺.

3.1.2. Synthesis of methyl 6-(2,6-dichloro-3,5-dimethoxyphenyl)-1*H*-indazole-4-carboxylate (**7**)

To a solution of methyl 6-bromo-1*H*-indazole-4-carboxylate (**5**) (10.0 g, 39.2 mmol) in 1,4-Dioxane (300 mL), Boc₂O (9.4 g, 43.1 mmol), Cs₂CO₃ (44.7 g, 137.2 mmol) were added into the reaction mixture, and the mixture was stirred at 25°C for 0.5 h. 2-(2,6-dichloro-3,5-dimethoxyphenyl)-4,4,5,5-tetramethyl-1,3,2-dioxaborolane (**6a**) (14.4 g, 43.1 mmol), Pd(dppf)Cl₂ (3.2 g, 3.92 mmol), H₂O (100 mL) was added into the reaction mixture and stirred at 100°C for 2 h under a nitrogen atmosphere. The reaction was cooled to 25°C. The aqueous phase was extracted with dichloromethane, and the combined organic phase were washed with water and brine, dried over Na₂SO₄, filtered and concentrated in vacuo. The resultant residue was purified by column chromatography to get the intermediate as a white solid (62.3%). ¹H NMR (400 MHz, Chloroform-*d*) δ 8.67 (s, 1H), 7.86 (s, 1H), 7.62 (s, 1H), 6.69 (s, 1H), 4.04 (s, 3H), 4.01 (s, 6H); (+) ESI-MS *m/z* 382 [M + H]⁺.

3.1.3. Synthesis of 6-(2,6-dichloro-3,5-dimethoxyphenyl)-1*H*-indazole-4-carboxylic acid (**8**)

To a solution of 6-(2,6-dichloro-3,5-dimethoxyphenyl)-*N*-phenyl-1*H*-indazole-4-carboxamide (**7**) (8.9 g, 23.35 mmol) in THF (120 mL), and Lithium hydroxide (3.92 g, 93.44 mmol) was dissolved into distilled water (30 mL) was added. Then, the mixture was stirred at 50°C for 6 h. The reaction was cooled to 25°C. The reaction mixture was acidified with 1N HCl and the solid product was filtered off, washed with water, and dried (76.2%). ¹H NMR (400 MHz, DMSO-*d*₆) δ 8.45 (s, 1H), 7.67 (d, *J* = 3.8 Hz, 1H), 7.54 (s, 1H), 7.03 (s, 1H), 4.05 – 3.94 (m, 6H); ¹³C NMR (126 MHz, Chloroform-*d*) δ 167.66, 154.10 (C×2), 139.64, 134.83, 127.43, 127.34 (C×2), 126.65, 126.27, 115.65, 114.23 (C×2), 96.58, 56.15 (C×2),. (+) ESI-MS *m/z* 368 [M + H]⁺.

3.1.4. Synthesis of

6-(2,6-dichloro-3,5-dimethoxyphenyl)-*N*-phenyl-1*H*-indazole-4-carboxamide (**10a-e,11a-e,12a-i**)

To a solution of 6-(2,6-dichloro-3,5-dimethoxyphenyl)-1*H*-indazole-4-carboxylic acid (**8**) (30 mg, 0.082 mmol) in pyridine (3 mL) at 0°C. POCl₃ (12 μl, 0.090 mmol) was added, the mixture was stirred at 0°C for 1 h. Aniline was added into the reaction mixture and stirred at 0°C for 10 min, then, the mixture was stirred at 25°C for 1.5 h. The reaction was quenched with distilled water, and the organic phase was washed with water, 1N HCl and brine, dried over Na₂SO₄, filtered and concentrated in vacuo. The resultant residue was purified by column chromatography to get the final product as a white solid.

6-(2,6-dichloro-3,5-dimethoxyphenyl)-*N*-phenyl-1*H*-indazole-4-carboxamide (**10a**). 82.3% yield; m.p. 115–117°C; ¹H NMR (400 MHz, Chloroform-*d*) δ 8.70 (s, 1H), 8.18 (s, 1H), 7.72 (d, *J* = 8.0 Hz, 2H), 7.56 (s, 1H), 7.49 (s, 1H), 7.40 (t, *J* = 7.7, 7.7 Hz, 2H), 6.66 (s, 1H), 3.99 (s, 6H). ¹³C NMR (126 MHz, Chloroform-*d*) δ 164.75, 154.64(2×C), 140.67, 139.94, 139.54, 137.76, 135.37, 135.21, 129.50, 129.14(2×C), 128.20, 124.73, 122.42, 121.71, 120.95, 120.35(2×C), 118.43, 118.38, 114.69, 114.56, 96.98, 56.64(2×CH₃). C₂₂H₁₇Cl₂N₃O₃(+) ESI-MS *m/z* 442 [M + H]⁺.

N-(3-acetylphenyl)-6-(2,6-dichloro-3,5-dimethoxyphenyl)-1*H*-indazole-4-carboxamide (**10b**). 78.4%

yield; ¹H NMR (400 MHz, Chloroform-*d*) δ 8.69 (s, 1H), 8.30 (s, 1H), 8.19 (t, *J* = 2.0, 2.0 Hz, 1H),

8.08 (ddd, $J = 8.1, 2.3, 1.0$ Hz, 1H), 7.75 (ddd, $J = 7.8, 1.7, 1.0$ Hz, 1H), 7.58 (s, 1H), 7.52 – 7.47 (m, 2H), 6.65 (s, 1H), 3.98 (s, 6H), 2.63 (s, 3H). ^{13}C NMR (126 MHz, Chloroform-*d*) δ 198.05, 154.73(2 \times C), 140.67, 139.95, 137.85, 135.39, 134.91, 130.01, 129.72, 129.48, 124.96, 124.85, 124.43, 121.82, 120.81, 119.84, 119.73, 114.90, 114.62, 97.11, 56.69(2 \times CH₃), 29.70. C₂₄H₁₉Cl₂N₃O₄(⁺) ESI-MS m/z 484 [M + H]⁺.

N-(4-acetylphenyl)-6-(2,6-dichloro-3,5-dimethoxyphenyl)-1H-indazole-4-carboxamide(**10c**). 76.3% yield; ^1H NMR (400 MHz, DMSO-*d*₆) δ 13.50 (s, 1H), 10.62 (s, 1H), 8.51 (s, 1H), 7.99 (s, 4H), 7.73 (s, 1H), 7.66 (s, 1H), 7.06 (s, 1H), 4.00 (s, 6H), 2.56 (s, 3H). ^{13}C NMR (126 MHz, DMSO-*d*₆) δ 197.12, 165.45, 154.96(2 \times C), 143.88, 140.02, 134.53, 134.33, 132.55, 130.10, 129.72(2 \times C), 127.20, 122.52, 122.90, 120.09(2 \times C), 116.85, 115.31, 113.61, 98.59, 57.29(2 \times CH₃), 26.96. C₂₄H₁₉Cl₂N₃O₄(⁺) ESI-MS m/z 484 [M + H]⁺.

6-(2,6-dichloro-3,5-dimethoxyphenyl)-*N*-(3-methoxyphenyl)-1H-indazole-4-carboxamide(**10d**). 78.6% yield; ^1H NMR (400 MHz, Chloroform-*d*) δ 8.68 (s, 1H), 8.10 (s, 1H), 7.55 (s, 1H), 7.46 (d, $J = 2.1$ Hz, 2H), 7.18 (d, $J = 8.3$ Hz, 1H), 6.72 (ddd, $J = 8.2, 2.6, 1.0$ Hz, 1H), 6.64 (s, 1H), 3.97 (s, 6H), 3.83 (s, 3H). ^{13}C NMR (126 MHz, Chloroform-*d*) δ 164.68, 160.27, 154.69 (2 \times C), 140.66, 139.90, 138.96, 135.48, 135.31, 129.82 (2 \times C), 128.27, 121.76, 120.93, 114.60(2 \times C), 112.38, 110.78, 105.84, 97.04, 56.66 (2 \times CH₃), 55.41. C₂₃H₁₉Cl₂N₃O₄ (⁺) ESI-MS m/z 472 [M + H]⁺.

6-(2,6-dichloro-3,5-dimethoxyphenyl)-*N*-(4-methoxyphenyl)-1H-indazole-4-carboxamide(**10e**). 72.5% yield; ^1H NMR (400 MHz, Chloroform-*d*) δ 8.69 (s, 1H), 7.89 (s, 1H), 7.60 (d, $J = 8.9$ Hz, 3H), 7.58 (d, $J = 1.2$ Hz, 1H), 7.47 – 7.45 (m, 1H), 6.95 (d, $J = 8.9$ Hz, 2H), 6.69 (s, 1H), 4.01 (s, 6H), 3.85 (d, $J = 1.0$ Hz, 3H). ^{13}C NMR (126 MHz, Chloroform-*d*) δ 164.61, 156.77, 154.72(2 \times C), 140.65, 139.98, 135.44, 130.76, 130.02, 129.74, 128.36, 122.21 (2 \times C), 121.64, 120.98, 114.65, 114.33(2 \times C), 97.07, 56.69(2 \times CH₃), 55.54. C₂₂H₁₈Cl₂N₄O₄ (⁺) ESI-MS m/z 473 [M + H]⁺.

6-(2,6-dichloro-3,5-dimethoxyphenyl)-*N*-(6-methoxypyridin-2-yl)-1H-indazole-4-carboxamide(**11a**). 71.5% yield; ^1H NMR (400 MHz, Chloroform-*d*) δ 8.72 (d, $J = 1.2$ Hz, 1H), 8.46 (s, 1H), 8.00 (d, $J = 7.8$ Hz, 1H), 7.70 (t, $J = 8.0, 8.0$ Hz, 1H), 7.62 (s, 1H), 7.54 (d, $J = 1.2$ Hz, 1H), 6.70 (s, 1H), 6.57 (d, $J = 8.1$ Hz, 1H), 4.02 (s, 6H), 3.91 (d, $J = 1.2$ Hz, 3H). ^{13}C NMR (126 MHz, Chloroform-*d*) δ 164.96, 162.93, 154.65(2 \times C), 149.00, 140.99, 140.77, 140.01, 135.31, 134.21, 127.41, 121.97(2 \times C), 120.45, 115.38, 114.62, 106.16, 106.00, 97.10, 56.63(2 \times CH₃), 53.50. C₂₂H₁₈Cl₂N₄O₄ (⁺) ESI-MS m/z 473 [M + H]⁺.

6-(2,6-dichloro-3,5-dimethoxyphenyl)-*N*-(2-methoxypyridin-4-yl)-1H-indazole-4-carboxamide(**11b**). 72.2% yield; ^1H NMR (400 MHz, Chloroform-*d*) δ 8.68 (s, 1H), 8.15 (d, $J = 5.7$ Hz, 1H), 8.05 (s, 1H), 7.62 (s, 1H), 7.46 (s, 1H), 7.22 (s, 1H), 7.20 (d, $J = 5.9$ Hz, 1H), 6.70 (s, 1H), 4.02 (s, 6H), 3.98 (s, 3H). ^{13}C NMR (126 MHz, Chloroform-*d*) δ 165.54, 164.88, 154.68(2 \times C), 147.75(2 \times C), 146.94, 140.68, 139.69, 135.41, 135.22, 127.35, 121.91, 120.93, 115.23, 114.49, 108.39, 99.85, 97.01, 56.64(2 \times CH₃), 53.68. C₂₂H₁₈Cl₂N₄O₄ (⁺) ESI-MS m/z 473 [M + H]⁺.

6-(2,6-dichloro-3,5-dimethoxyphenyl)-*N*-(4-methoxypyridin-2-yl)-1H-indazole-4-carboxamide(**11c**). 68.2% yield; ^1H NMR (400 MHz, Chloroform-*d*) δ 8.72 (s, 1H), 8.12 (d, $J = 6.4$ Hz, 1H), 8.10 (d, $J = 1.6$ Hz, 1H), 7.61 (s, 1H), 7.54 (s, 1H), 6.70 (s, 1H), 6.67 (dd, $J = 6.0, 1.8$ Hz, 1H), 4.02 (s, 6H), 3.97 (s, 3H). ^{13}C NMR (126 MHz, Chloroform-*d*) δ 167.67, 164.98, 154.70(2 \times C), 153.10, 148.41, 140.68, 139.83, 135.62, 135.26, 127.54, 123.47, 122.34, 120.90, 114.96, 114.69, 108.05, 98.94, 97.25, 56.71, 55.52(2 \times CH₃). C₂₂H₁₈Cl₂N₄O₄ (⁺) ESI-MS m/z 473 [M + H]⁺.

6-(2,6-dichloro-3,5-dimethoxyphenyl)-*N*-(6-methoxypyrimidin-4-yl)-1H-indazole-4-carboxamide (**11d**). 65.5% yield; ^1H NMR (400 MHz, Chloroform-*d*) δ 8.71 (s, 2H), 8.52 (s, 1H), 7.83 (s, 2H), 7.64 (s, 1H), 7.52 (s, 1H), 6.71 (s, 1H), 4.05 (s, 3H), 4.02 (s, 6H). ^{13}C NMR (126 MHz, Chloroform-*d*) δ 171.44, 165.06, 157.70, 157.58, 154.77(2 \times C), 140.71, 139.60, 135.59, 135.30, 126.67, 122.39, 120.87, 115.43, 114.63, 97.28, 95.35, 56.72(2 \times C), 54.30, 53.43. C₂₁H₁₇Cl₂N₅O₄ (⁺) ESI-MS m/z 474 [M + H]⁺.

6-(2,6-dichloro-3,5-dimethoxyphenyl)-*N*-(2-methoxypyrimidin-4-yl)-1H-indazole-4-carboxamide (**11e**). 66.6% yield; ^1H NMR (400 MHz, Chloroform-*d*) δ 8.75 (s, 1H), 8.41 (d, $J = 5.7$ Hz, 1H), 7.63 (s, 1H), 7.52 (s, 1H), 6.70 (s, 1H), 6.52 (d, $J = 5.8$ Hz, 1H), 4.01 (s, 6H), 3.99 (s, 3H). ^{13}C NMR (126

MHz, Chloroform-*d*) δ 170.41, 163.90, 158.20, 157.11, 154.74(2 \times C), 140.70, 139.84, 135.57, 135.42, 127.55, 122.29, 121.15, 115.19, 114.68(2 \times C), 104.12, 97.15, 56.70 (2 \times CH₃), 54.04. C₂₁H₁₇Cl₂N₅O₄ (+) ESI-MS *m/z* 474 [M + H]⁺.

methyl 3-(6-(2,6-dichloro-3,5-dimethoxyphenyl)-1H-indazole-4-carboxamido)benzoate(12a). 63.5% yield; ¹H NMR (400 MHz, Chloroform-*d*) δ 8.70 (s, 1H), 8.20 (s, 1H), 8.11 (d, *J* = 8.3 Hz, 1H), 8.04 (s, 1H), 7.88 (d, *J* = 8.0 Hz, 1H), 7.62 (s, 1H), 7.53 – 7.47 (m, 2H), 6.71 (s, 1H), 4.02 (s, 6H), 3.96 (s, 3H).

¹³C NMR (126 MHz, Chloroform-*d*) δ 166.67, 164.81, 154.71(2 \times C), 140.70, 139.84, 138.01, 135.46, 135.28, 131.04, 130.02, 129.73, 129.34, 127.82, 125.75, 124.76, 121.84, 121.12, 114.84, 114.58, 97.08, 56.67(2 \times CH₃), 52.30. C₂₄H₁₉Cl₂N₃O₅ (+) ESI-MS *m/z* 500 [M + H]⁺.

6-(2,6-dichloro-3,5-dimethoxyphenyl)-N-(3-(methylcarbamoyl)phenyl)-1H-indazole-4-carboxamide (12b). 62.4% yield; m.p. 155-157°C; ¹H NMR (400 MHz, Chloroform-*d*) δ 8.68 (s, 1H), 8.17 (s, 2H), 7.85 (d, *J* = 8.3 Hz, 1H), 7.61 (d, *J* = 8.9 Hz, 2H), 7.49 (d, *J* = 4.6 Hz, 1H), 6.70 (s, 1H), 4.02 (s, 6H), 3.05 (d, *J* = 4.8 Hz, 3H). ¹³C NMR (126 MHz, Chloroform-*d*) δ 167.78, 164.97, 154.70(2 \times C), 140.71, 139.83, 138.19, 135.52, 135.46, 135.11, 129.49, 127.71, 123.08, 122.96, 122.06, 120.81, 118.56(2 \times C), 114.89, 114.58, 97.09, 56.67(2 \times CH₃), 26.92. C₂₄H₂₀Cl₂N₄O₄ (+) ESI-MS *m/z* 499 [M + H]⁺.

ethyl 3-(6-(2,6-dichloro-3,5-dimethoxyphenyl)-1H-indazole-4-carboxamido)benzoate(12c). 61.5% yield; ¹H NMR (400 MHz, Chloroform-*d*) δ 8.71 (s, 1H), 8.29 (s, 1H), 8.19 (t, *J* = 1.9, 1.9 Hz, 1H), 8.15 (d, *J* = 8.4 Hz, 1H), 7.86 (dt, *J* = 7.8, 1.4, 1.4 Hz, 1H), 7.59 (d, *J* = 1.2 Hz, 1H), 7.52 – 7.46 (m, 2H), 6.66 (s, 1H), 4.40 (q, *J* = 7.3, 7.3, 7.3 Hz, 2H), 3.99 (s, 6H), 1.41 (t, *J* = 7.1, 7.1 Hz, 3H). ¹³C NMR (126 MHz, Chloroform-*d*) δ 166.13, 164.78, 154.74(2 \times C), 139.84, 137.91, 135.51, 131.42, 129.32(2 \times C), 127.87, 125.76, 125.02, 124.71(2 \times C), 121.86, 121.06, 114.76, 114.62(2 \times C), 97.12, 61.23, 56.69(2 \times CH₃), 14.34. C₂₅H₂₁Cl₂N₃O₅ (+) ESI-MS *m/z* 514 [M + H]⁺.

6-(2,6-dichloro-3,5-dimethoxyphenyl)-N-(3-nitrophenyl)-1H-indazole-4-carboxamide(12d). 62.2% yield; ¹H NMR (400 MHz, DMSO-*d*₆) δ 13.51 (s, 1H), 10.75 (s, 1H), 8.83 (s, 1H), 8.54 (s, 1H), 8.27 (d, *J* = 8.2 Hz, 1H), 7.99 (d, *J* = 8.6 Hz, 1H), 7.75 (s, 1H), 7.70 – 7.65 (m, 2H), 7.07 (s, 1H), 4.00 (s, 6H).

¹³C NMR (126 MHz, DMSO-*d*₆) δ 165.56, 154.97(2 \times C), 148.35, 140.86, 140.67, 140.00, 134.59, 134.44, 130.50, 126.87, 126.79, 122.48, 120.92, 118.67, 115.43, 115.02, 113.62, 98.61, 57.30, 55.37(C \times CH₃). C₂₂H₁₆Cl₂N₄O₅ (+) ESI-MS *m/z* 487 [M + H]⁺.

6-(2,6-dichloro-3,5-dimethoxyphenyl)-N-(3-(3-methyl-2-oxoimidazolidin-1-yl)phenyl)-1H-indazole-4-carboxamide(12e). 63.3% yield; ¹H NMR (400 MHz, Chloroform-*d*) δ 8.48 (d, *J* = 1.0 Hz, 1H), 8.28 (s, 1H), 8.00 (t, *J* = 2.1, 2.1 Hz, 1H), 7.57 – 7.53 (m, 2H), 7.49 (s, 1H), 7.45 (d, *J* = 1.1 Hz, 1H), 7.32 (t, *J* = 8.2, 8.2 Hz, 1H), 7.22 (dd, *J* = 7.9, 1.6 Hz, 2H), 6.65 (s, 1H), 3.98 (s, 6H), 3.89 – 3.83 (m, 2H), 3.52 – 3.47 (m, 2H), 2.90 (s, 3H). ¹³C NMR (126 MHz, Chloroform-*d*) δ 164.92, 158.18, 154.66(2 \times C), 141.11, 140.66, 140.00, 138.50, 135.46, 135.05, 129.46, 128.28, 121.99, 120.75, 114.71, 114.52, 114.31, 113.12, 109.33(2 \times C), 97.15, 56.69(2 \times CH₃), 42.43, 31.22, 29.70. C₂₆H₂₃Cl₂N₅O₄ (+) ESI-MS *m/z* 540 [M + H]⁺.

6-(2,6-dichloro-3,5-dimethoxyphenyl)-N-(3-morpholinophenyl)-1H-indazole-4-carboxamide(12f). 64.8% yield; m.p. 159-161°C; ¹H NMR (400 MHz, Chloroform-*d*) δ 8.69 (s, 1H), 8.07 (s, 1H), 7.57 (s, 1H), 7.52 (t, *J* = 2.1, 2.1 Hz, 1H), 7.47 (d, *J* = 1.1 Hz, 1H), 7.06 (dd, *J* = 8.2, 1.2 Hz, 1H), 6.73 (dd, *J* = 8.2, 2.4 Hz, 1H), 6.67 (s, 1H), 4.00 (s, 6H), 3.91 – 3.85 (m, 4H), 3.25 – 3.19 (m, 4H). ¹³C NMR (126 MHz, Chloroform-*d*) δ 164.75, 154.64 (2 \times C), 152.08, 140.67, 139.93, 138.79, 135.39, 135.23, 129.66(2 \times C), 128.33, 121.70, 120.91, 114.63, 114.54, 111.94, 111.64, 107.60, 96.97, 66.88(2 \times CH₂), 56.63(2 \times CH₃), 49.17 (2 \times CH₂). C₂₆H₂₄Cl₂N₄O₄ (+) ESI-MS *m/z* 527 [M + H]⁺.

6-(2,6-dichloro-3,5-dimethoxyphenyl)-N-(3-(piperazin-1-yl)phenyl)-1H-indazole-4-carboxamide(12g). 60.5% yield; m.p. 221-223°C; ¹H NMR (400 MHz, DMSO-*d*₆) δ 13.48 (s, 1H), 10.21 (s, 1H), 8.49 (s, 1H), 7.67 (s, 1H), 7.63 (s, 1H), 7.51 (s, 1H), 7.36 (d, *J* = 8.0 Hz, 1H), 7.24 (t, *J* = 8.0, 8.0 Hz, 1H), 7.06 (s, 1H), 6.78 (d, *J* = 8.2 Hz, 1H), 4.00 (s, 6H), 3.23 (s, 4H), 3.17 (d, *J* = 5.2 Hz, 4H). ¹³C NMR (126 MHz, Chloroform-*d*) δ 154.60(2 \times C), 150.89, 140.75, 139.27, 139.06, 135.25, 130.09, 129.98,

129.76(2×C), 128.04, 121.75, 120.56, 115.03, 114.51, 114.00, 113.17, 109.09, 97.00, 56.6(2×CH₃), 47.36(2×CH₂), 43.77(2×CH₂). C₂₆H₂₅Cl₂N₅O₃ (+) ESI-MS m/z 526 [M + H]⁺.

6-(2,6-dichloro-3,5-dimethoxyphenyl)-N-(3-(1-methyl-1H-pyrazol-4-yl)phenyl)-1H-indazole-4-carboxamide (**12h**). 68.8% yield; m.p. 188-190°C; ¹H NMR (400 MHz, Chloroform-*d*) δ 8.29 (s, 1H), 7.91 (s, 1H), 7.78 (s, 1H), 7.67 (s, 1H), 7.56 (s, 1H), 7.52 (s, 2H), 7.39 (m, 1H), 7.36 (d, *J* = 7.9 Hz, 1H), 3.97 (s, 6H), 3.94 (s, 3H). ¹³C NMR (126 MHz, DMSO-*d*₆) δ 165.10, 154.95(2×C), 140.86, 140.14, 139.90, 136.35, 134.59, 133.42, 131.09, 129.54, 129.00, 128.90, 128.28, 127.66, 122.33, 122.23, 121.06, 118.79, 117.59, 114.88, 113.63, 98.55, 57.29(2×CH₃), 39.12. C₂₆H₂₁Cl₂N₅O₃ (+) ESI-MS m/z 522 [M + H]⁺.

6-(2,6-dichloro-3,5-dimethoxyphenyl)-N-(3-(pyrimidin-5-yl)phenyl)-1H-indazole-4-carboxamide (**12i**). 67.6% yield; m.p. 177-179°C; ¹H NMR (400 MHz, Chloroform-*d*) δ 9.20 (s, 1H), 8.97 (s, 2H), 8.69 (s, 1H), 8.40 (s, 1H), 8.05 (s, 1H), 7.79 – 7.73 (m, 1H), 7.57 (s, 1H), 7.53 (d, *J* = 7.9 Hz, 1H), 7.50 (s, 1H), 7.36 (d, *J* = 7.7 Hz, 1H), 3.96 (s, 6H). ¹³C NMR (126 MHz, DMSO-*d*₆) δ 165.25, 157.86, 155.15(2×C), 154.96(2×C), 140.86, 140.34, 140.10, 134.66, 134.59, 134.50, 133.79, 130.16, 127.44, 122.82, 122.29, 121.31, 120.96, 119.43, 115.05, 113.63(2×C), 98.56, 57.29(2×CH₃). C₂₆H₁₉Cl₂N₅O₃ (+) ESI-MS m/z 520 [M + H]⁺.

3.1.6. Synthesis of
6-(2,6-dichloro-3,5-dimethoxyphenyl)-N-(3-(4-piperazin-1-yl)phenyl)-1H-indazole-4-carboxamide (**13a-e**)

To a solution of 6-(2,6-dichloro-3,5-dimethoxyphenyl)-1H-indazole-4-carboxylic acid (**8**) in dry DCM, DIPEA and HATU were added and the mixture was stirred at 25°C for 1-4 h. 3-(4-ethylpiperazin-1-yl)aniline (**9a-e**) was then added and the mixture was stirred at 25°C for 0.5 h. The reaction was quenched with distilled water, and the organic phase was washed with water and brine, dried over Na₂SO₄, filtered and concentrated in vacuo.

6-(2,6-dichloro-3,5-dimethoxyphenyl)-N-(3-(4-methylpiperazin-1-yl)phenyl)-1H-indazole-4-carboxamide (**13a**). 60.7% yield; m.p. 205-207°C; ¹H NMR (400 MHz, Chloroform-*d*) δ 8.68 (s, 1H), 7.92 (s, 1H), 7.59 (s, 1H), 7.48 (s, 1H), 7.46 (s, 1H), 7.05 (d, *J* = 8.8 Hz, 1H), 6.76 (d, *J* = 8.5 Hz, 1H), 6.69 (s, 1H), 4.02 (s, 6H), 3.39 – 3.31 (m, 4H), 2.77 – 2.68 (m, 4H), 2.46 (s, 3H). C₂₇H₂₇Cl₂N₅O₃ (+) ESI-MS m/z 540 [M + H]⁺.

6-(2,6-dichloro-3,5-dimethoxyphenyl)-N-(3-(4-ethylpiperazin-1-yl)phenyl)-1H-indazole-4-carboxamide (**13b**). 60.3% yield; ¹H NMR (400 MHz, Chloroform-*d*) δ 8.67 (s, 1H), 7.97 (s, 1H), 7.60 (s, 1H), 7.49 (s, 1H), 7.46 (s, 1H), 7.07 (dd, *J* = 8.5, 1.4 Hz, 1H), 6.74 (dd, *J* = 8.6, 2.3 Hz, 1H), 6.69 (s, 1H), 4.01 (s, 6H), 3.47 – 3.38 (m, 4H), 2.83 (s, 4H), 2.74 – 2.65 (m, 2H), 0.90 (t, *J* = 6.8, 6.8 Hz, 3H). ¹³C NMR (126 MHz, Chloroform-*d*) δ 164.72, 154.72(2×C), 140.65, 139.93, 138.73, 135.48, 135.26, 130.49, 129.74(2×C), 128.36, 121.76, 120.90, 114.64, 114.53(2×C), 112.43, 111.77, 108.23, 97.08, 67.10, 56.69(2×C), 52.33, 52.24, 48.18, 14.13. C₂₈H₂₉Cl₂N₅O₃ (+) ESI-MS m/z 554 [M + H]⁺.

N-(3-(4-allylpiperazin-1-yl)phenyl)-6-(2,6-dichloro-3,5-dimethoxyphenyl)-1H-indazole-4-carboxamide (**13c**). 56.2% yield; ¹H NMR (400 MHz, Chloroform-*d*) δ 8.68 (s, 1H), 7.92 (s, 1H), 7.59 (s, 1H), 7.46 (s, 2H), 7.10 – 7.02 (m, 1H), 6.75 (d, *J* = 8.5 Hz, 1H), 6.72 (s, 1H), 5.96 (m, 1H), 5.30 – 5.22 (m, 2H), 4.05 – 3.99 (m, 6H), 3.39 – 3.31 (m, 4H), 3.21 – 3.12 (m, 2H), 2.78 – 2.67 (m, 4H). C₂₉H₂₉Cl₂N₅O₃(+) ESI-MS m/z 566 [M + H]⁺.

6-(2,6-dichloro-3,5-dimethoxyphenyl)-N-(3-(4-isopropylpiperazin-1-yl)phenyl)-1H-indazole-4-carboxamide (**13d**). 55.6% yield; ¹H NMR (400 MHz, Chloroform-*d*) δ 8.67 (s, 1H), 7.97 (s, 1H), 7.60 (s, 1H), 7.49 (s, 1H), 7.01 (t, *J* = 8.0, 8.0 Hz, 1H), 6.43 – 6.35 (m, 2H), 6.32 (d, *J* = 8.0 Hz, 1H), 3.99 (s, 6H), 3.47 – 3.38 (m, 4H), 2.48 (s, 4H), 1.31 (s, 1H), 1.26 (d, *J* = 6.6 Hz, 6H). C₂₉H₃₁Cl₂N₅O₃(+) ESI-MS m/z 568 [M + H]⁺.

N-(3-(4-acetylpiperazin-1-yl)phenyl)-6-(2,6-dichloro-3,5-dimethoxyphenyl)-1H-indazole-4-carboxamide (**13e**). 65.8% yield; m.p. 209-211°C; ¹H NMR (400 MHz, Chloroform-*d*) δ 8.68 (s, 1H), 8.06 (s, 1H), 7.59 (s, 1H), 7.54 (s, 1H), 7.47 (s, 1H), 7.06 (d, *J* = 7.6 Hz, 1H), 6.75 (d, *J* = 10.9 Hz, 1H), 6.68 (s, 1H), 4.01 (s, 6H), 3.81 – 3.76 (m, 2H), 3.67 – 3.62 (m, 2H), 3.51 (s, 3H), 3.30 – 3.24 (m, 2H), 3.24 – 3.19 (m, 1H). ¹³C NMR (126 MHz, Chloroform-*d*) δ 169.10, 164.75, 154.71(2×C), 151.71,

140.67, 139.92, 138.81, 135.46, 135.27, 129.75, 128.30, 121.75, 120.91, 114.59(2×C), 112.75, 111.99, 108.48, 97.05, 56.68(2×CH₃), 49.43, 49.18, 46.18, 41.33, 21.37. C₂₈H₂₇Cl₂N₅O₄⁽⁺⁾ ESI-MS m/z 568 [M + H]⁺.

3.2 Molecular docking

The structure of human FGFR1 kinase domain with its inhibitor NVP-BGJ398 (ID: 3TT0) was downloaded from PDB database. Two compounds (**4** and **10a**) were docked into FGFR1 ATP site using Glide with XP mode. The protein structure was prepared using Protein preparation wizard tool in Maestro, which fixed the protein structure by verifying proper assignment of bonds, adding hydrogens, deleting all water molecules and refining hydrogen atoms. The binding pattern of NVP-BGJ398 to FGFR1 was used as reference to define the active site and docking grids within a 14×14 ×14 Å box. All the docking parameters were set as default values in Glide software. Only the best scored conformation was selected for visualization with Pymol software.

3.3 Elisa kinase assay

The effects of compounds on the activities of FGFR1 kinases were determined using enzyme-linked immunosorbent assays (ELISAs) with purified recombinant proteins. Briefly, 20 µg/mL poly (Glu, Tyr)_{4:1} (Sigma, St Louis, MO, USA) was pre-coated in 96-well plates as a substrate. A 50-µL aliquot of 10 µmol/L ATP solution diluted in kinase reaction buffer (50 mmol/L HEPES [pH 7.4], 50 mmol/L MgCl₂, 0.5 mmol/L MnCl₂, 0.2 mmol/L Na₃VO₄, and 1 mmol/L DTT) was added to each well; 1 µL of various concentrations of compounds diluted in 1% DMSO (*v/v*) (Sigma, St Louis, MO, USA) were then added to each reaction well. DMSO (1%, *v/v*) was used as the negative control. The kinase reaction was initiated by the addition of purified tyrosine kinase proteins diluted in 49 µL of kinase reaction buffer. After incubation for 60 min at 37°C, the plate was washed three times with phosphate-buffered saline (PBS) containing 0.1% Tween 20 (T-PBS). Anti-phosphotyrosine (PY99) antibody (100 µL; 1:500, diluted in 5 mg/mL BSA T-PBS) was then added. After a 30-min incubation at 37°C, the plate was washed three times, and 100 µL horseradish peroxidase-conjugated goat anti-mouse IgG (1:2000, diluted in 5 mg/mL BSA T-PBS) was added. The plate was then incubated at 37°C for 30 min and washed 3 times. A 100-µL aliquot of a solution containing 0.03% H₂O₂ and 2 mg/mL *o*-phenylenediamine in 0.1 mol/L citrate buffer (pH 5.5) was added. The reaction was terminated by the addition of 50 µL of 2 mol/L H₂SO₄ as the color changed, and the plate was analyzed using a multi-well spectrophotometer (SpectraMAX 190, from Molecular Devices, Palo Alto, CA, USA) at 490 nm. The inhibition rate (%) was calculated using the following equation: $[1 - (A_{490}/A_{490 \text{ control}})] \times 100\%$. The IC₅₀ values were calculated from the inhibition curves in two separate experiments.

Conclusions

In summary, we reported the design, synthesis, and biological evaluation of a novel series of 6-(2,6-dichloro-3,5-dimethoxyphenyl)-4-Substituted-1*H*-indazole derivatives as potent FGFR kinase inhibitors. Through four rounds of optimization, compound **13a** stood out as the most potent FGFR1 inhibitor with the inhibition potency (IC₅₀=30.2±1.9 nM). We think current study not only provided potent FGFR inhibitors for the community, it also pointed a new direction for optimize this promising scaffold.

Acknowledgements

We are grateful for financial support from The Foundation of China Postdoctoral Science (Grant No. 2015M580370); the National Natural Science Foundation of China (Grant No. 81473243); Youth Innovation Promotion Association and the "Personalized Medicines—Molecular Signature-based Drug Discovery and Development", Strategic Priority Research Program of the Chinese Academy of Sciences, Grant No. XDA12020317); the

program for Innovative Research Team of the Ministry of Education and Program for Liaoning Innovative Research Team in University.

Author Contributions: Bing Xiong, Yuchi Ma, Jing Ai and Dongmei Zhao designed the research; Zhen Zhang, Yang Dai conducted the research; Maosheng Cheng, Meiyu Geng, Jingkang Shen analyzed the data; Bing Xiong, Yuchi Ma, Jing Ai wrote the paper.

Conflicts of Interest: The authors declare no conflict of interest.

References

- (1) Carter, E.P.; Fearon, A.E.; Grose, R.P. Careless talk costs lives: fibroblast growth factor receptor signalling and the consequences of pathway malfunction. *Trends Cell Biol.* **2015**, *25*, 221–233. <http://www.sciencedirect.com/science/article/pii/S0962892414001962>
- (2) Laestander, C.; Engström, W. Role of fibroblast growth factors in elicitation of cell responses. *Cell Proliferation* **2014**, *47*, 3–11. <http://onlinelibrary.wiley.com/doi/10.1111/cpr.12084/abstract;jsessionid=D8B11701E115A074405C9082FAC53357.f03t04>
- (3) Brooks, A.N.; Kilgour, E.; Smith, P.D. Molecular Pathways: Fibroblast Growth Factor Signaling: A New Therapeutic Opportunity in Cancer. *Clin. Cancer Res.* **2012**, *18*, 1855–1862. <http://clincancerres.aacrjournals.org/content/18/7/1855.long>
- (4) Shaw, A.T.; Kim, D.W.; Nakagawa, K.; Seto, T. et al. Crizotinib versus chemotherapy in advanced ALK-positive lung cancer. *N. Engl. J. Med.* **2013**, *368*, 2385–2394. <http://www.nejm.org/doi/full/10.1056/NEJMoa1214886>
- (5) Parker, B.C.; Annala, M.J.; Cogdell, D.E.; Granberg, K.J.; Sun, Y.; Ji, P. et al. The tumorigenic FGFR3–TACC3 gene fusion escapes miR-99a regulation in glioblastoma. *J. Clin. Invest.* **2013**, *123*, 855–865. <http://www.jci.org/articles/view/67144>
- (6) Singh, D.; Chan, J.M.; Zoppoli, P.; Niola, F.; Sullivan, R.; Castano, A. et al. Transforming fusions of FGFR and TACC genes in human glioblastoma. *Science* **2012**, *337*, 1231–1235. <http://science.sciencemag.org/content/337/6099/1231>
- (7) Wang, R.; Wang, L.; Li, Y.; Hu, H.; Shen, L.; Shen, X. et al. FGFR1/3 tyrosine kinase fusions define a unique molecular subtype of non-small cell lung cancer. *Clin. Cancer Res.* **2014**, *1*, 4107–4114. <http://clincancerres.aacrjournals.org/content/20/15/4107.long>
- (8) Touat, M.; Ileana, E.; Postel-Vinay, S.; André, F.; Soria, J. C. Targeting FGFR signaling in cancer. *Clin. Cancer Res.* **2015**, *21*, 2684–2694. <http://clincancerres.aacrjournals.org/content/21/12/2684.long>
- (9) Eswarakumar, V. P.; Lax, I.; Schlessinger, J. Cellular signaling by fibroblast growth factor receptors. *Cytokine Growth Factor Rev.* **2005**, *16*, 139–149. [http://www.cgfr.co.uk/article/S1359-6101\(05\)00002-X/fulltext](http://www.cgfr.co.uk/article/S1359-6101(05)00002-X/fulltext)
- (10) Turner, N.; Grose, R. Fibroblast growth factor signalling: from development to cancer. *Nat. Rev. Cancer* **2010**, *10*, 116–129. <http://www.nature.com/nrc/journal/v10/n2/abs/nrc2780.html>
- (11) Dieci, M. V.; Arnedos, M.; André, F.; Soria, J. C. Fibroblast Growth Factor Receptor Inhibitors as a Cancer Treatment: From a Biologic Rationale to Medical Perspectives. *Cancer Discovery* **2013**, *3*, 264–279. <http://cancerdiscovery.aacrjournals.org/content/3/3/264.long>
- (12) Hallinan, N.; Finn, S.; Cuffe, S.; Rafee, S.; O'Byrne, K.; Gately, K. Targeting the fibroblast growth factor receptor family in cancer. *Cancer Treat Rev.* **2016**, *46*, 51–62. <http://www.sciencedirect.com/science/article/pii/S0305737216300135>
- (13) Ronca, R.; Giacomini, A.; Rusnati, M.; Presta, M. The potential of fibroblast growth factor/fibroblast growth factor receptor signaling as a therapeutic target in tumor angiogenesis. *Expert Opin. Ther. Targets* **2015**, *19*, 1361–1377. <http://www.ncbi.nlm.nih.gov/pubmed/26125971>
- (14) Singh, D.; Chan, J. M.; Zoppoli, P.; Niola, F.; Sullivan, R. et al. Transforming Fusions of

- FGFR and TACC Genes in Human Glioblastoma. *Science* **2012**, *337*, 1231-1235. <https://www.ncbi.nlm.nih.gov/pmc/articles/PMC3677224/>
- (15) Tanner, Y.; Grose, R.P. Dysregulated FGF signalling in neoplastic disorders. *Semin. Cell Dev. Biol.* **2016**, *53*, 126-135. <http://www.ncbi.nlm.nih.gov/pubmed/26463732>
- (16) Lemieux, S.; Hadden, M. K. Targeting the fibroblast growth factor receptors for the treatment of cancer. *Anti-Cancer Agents Med. Chem.* **2013**, *13*, 748-761. <http://www.ncbi.nlm.nih.gov/pubmed/23272905>
- (17) Izzedine, H.; Ederhy, S.; Goldwasser, F.; Soria, J. C.; Milano, G.; Cohen, A.; Khayat, D.; Spano, J. P. Management of hypertension in angiogenesis inhibitor-treated patients. *Ann. Oncol.* **2009**, *20*, 807-815. <http://annonc.oxfordjournals.org/content/20/5/807.long>
- (18) Ricciardi, S.; Tomao, S.; de Marinis, F. Toxicity of targeted therapy in non-small-cell lung cancer management. *Clin. Lung Cancer* **2009**, *10*, 28-35. <http://www.ncbi.nlm.nih.gov/pubmed/19289369>
- (19) Bahleda, R.; Dienstmann, R.; Adamo, B.; Gazzah, A.; Infante, J.R.; Zhong, B. et al. Phase 1 study of JNJ-42756493, a pan-fibroblast growth factor receptor (FGFR) inhibitor, in patients with advanced solid tumors. *J. Clin. Oncol.* **2015**, *33*, 3401-3408. <http://jco.ascopubs.org/content/33/30/3401.long>
- (20) Gavine, P. R.; Mooney, L.; Kilgour, E.; Thomas, A. P.; Al-Kadhimi, K.; Beck, S.; Rooney, C.; Coleman, T.; Baker, D.; Mellor, M. J.; Brooks, A. N.; Klinowska, T. AZD4547: an orally bioavailable, potent, and selective inhibitor of the fibroblast growth factor receptor tyrosine kinase family. *Cancer Res.* **2012**, *72*, 2045-2056. <http://www.ncbi.nlm.nih.gov/pubmed/22369928>
- (21) Guagnano, V.; Furet, P.; Spanka, C.; Bordas, V.; Le Douget, M.; Stamm, C.; Brueggen, J.; Jensen, M. R.; Schnell, C.; Schmid, H.; Wartmann, M.; Berghausen, J.; Drueckes, P.; Zimmerlin, A.; Bussiere, D.; Murray, J.; Graus Porta, D. Discovery of 3-(2,6-dichloro-3,5-dimethoxy-phenyl)-1-[6-[4-(4-ethyl-piperazin-1-yl)-phenylamino]-pyrimidin-4-yl]-1-methyl-urea (NVP-BGJ398), a potent and selective inhibitor of the fibroblast growth factor receptor family of receptor tyrosine kinase. *J. Med. Chem.* **2011**, *54*, 7066-7083. <http://www.ncbi.nlm.nih.gov/pubmed/21936542>
- (22) Liu, J.; Peng, X.; Dai, Y.; Zhang, W.; Ren, S. M.; Ai, J.; Geng, M. Y.; Li, Y. X. Design, synthesis and biological evaluation of novel FGFR inhibitors bearing an indazole scaffold. *Org. Biomol. Chem.* **2015**, *13*, 7643-7654. <http://www.ncbi.nlm.nih.gov/pubmed/26080733>
- (23) Zhao, B.; Li, Y. X.; Xu, P.; Dai, Y.; Luo, C.; Sun, Y. M.; Ai, J.; Geng, M. Y.; Duan, W. H. Discovery of substituted 1*H*-pyrazolo[3,4-*b*]pyridine derivatives as potent and selective FGFR kinase inhibitors. *ACS. Med. Chem. Lett.* **2016**, *7*, 629-634. <http://www.ncbi.nlm.nih.gov/pubmed/27326339>

Sample Availability: Samples of the compounds are available from the authors.



© 2016 by the authors; licensee Preprints, Basel, Switzerland. This article is an open access article distributed under the terms and conditions of the Creative Commons by Attribution (CC-BY) license (<http://creativecommons.org/licenses/by/4.0/>).